siRNA-Mediated Down-regulation of Ceramide Synthase 1 Leads to Apoptotic Resistance in Human Head and Neck Squamous Carcinoma Cells after Photodynamic Therapy

DUSKA SEPAROVIC[1,2], PAUL BREEN[1*], NICHOLAS JOSEPH[1*], JACEK BIELAWSKI[3], JASON S. PIERCE[3], ERIC VAN BUREN[2] and TATYANA I. GUDZ[4,5]

[1]*Department of Pharmaceutical Sciences, Eugene Applebaum College of Pharmacy and Health Sciences, and* [2]*Karmanos Cancer Institute, Wayne State University, Detroit, MI, USA;* [3]*Department of Biochemistry and Molecular Biology,* [4]*Ralph H. Johnson Veterans Affairs Medical Center, and* [5]*Department of Neuroscience, Medical University of South Carolina Charleston, SC, U.S.A.*

Abstract. *Background: The effectiveness of photodynamic therapy (PDT) for cancer treatment correlates with apoptosis. We previously observed that the knockdown of ceramide synthase 6, an enzyme from the de novo sphingolipid biosynthesis pathway, is associated with marked reduction in C18-dihydroceramide and makes cells resistant to apoptosis post-PDT. Down-regulation of ceramide synthase 1 (CERS1) can also render cells resistant to anticancer drugs. Aim: To explore the impact of CERS1 knockdown on apoptosis and the sphingolipid profile, post-PDT, with the silicone phthalocyanine Pc 4, in a human head and neck squamous carcinoma cell line. Materials and Methods: Besides siRNA transfection and PDT treatment, the following methods were used: immunoblotting for protein expression, mass spectrometry for sphingolipid analysis, spectroflurometry and flow cytometry for apoptosis detection, and trypan blue assay for cell viability evaluation. Results: CERS1 knockdown led to inhibition of PDT-induced caspase 3-like (DEVDase) activation, of apoptosis and cell death. CERS1 knockdown was associated with global and selective decreases in ceramides and dihydroceramides, in particular C18-, C18:1- and C20-ceramide post-PDT. Conclusion: Our novel findings are consistent with the notion that CERS1 regulates apoptotic resistance to PDT, partly via C18- and C20-ceramide, and that CERS1 is a molecular target for controlling resistance to PDT.*

Production of the sphingolipid ceramide is associated with apoptosis (1-3). Ceramide can be generated *via* the *de novo* sphingolipid biosynthesis pathway (Figure 1), in which ceramide synthase (CERS) acylates dihydrosphingosine to give rise to dihydroceramide, which is then converted to ceramide. Six mammalian CERSs have been characterized with different yet overlapping fatty acyl CoA specificity (4-8). CERSs have been implicated in different biological functions (1, 2, 9). CERS1 is involved in C18-ceramide synthesis (10). The enzyme has been implicated in sensitization of cells to chemotherapeutic agents (11, 12). siRNA-mediated down-regulation of CERS1 inhibits imatinib-induced cell death (13). Unlike in non-squamous tumors, in head and neck cancer, reduced CERS1 expression correlates with lower C18-ceramide levels compared to normal tissue (14). Overexpression of CERS1 in head and neck squamous carcinoma cells is associated with the generation of C18-ceramide and promotion of apoptosis. In contrast, *CERS1* knockdown renders the cells resistant to anticancer agents (12).

The *de novo* sphingolipid biosynthesis pathway modulates apoptosis after photodynamic therapy (PDT) (15-17). PDT utilizes a light-absorbing photosensitizer, visible light and oxygen to generate reactive oxygen species that can destroy malignant cellular targets by apoptosis (18). The efficacy of PDT correlates with tumor cell apoptosis (19). We have demonstrated that *de novo* sphingolipids affect apoptosis after PDT with the silicone phthalocyanine photosensitizer Pc 4 (15-17). We have recently shown that the knockdown of ceramide synthase 6 *(CERS6)* is associated with marked reduction in C18-dihydroceramide and renders cells resistant to apoptosis post-PDT (20). However, the role of CERS1 in

*These Authors contributed equally in this study.

Correspondence to: Duska Separovic, Department of Pharmaceutical Sciences, Eugene Applebaum College of Pharmacy and Health Sciences, Wayne State University, 259 Mack Ave., Detroit, MI 48201, U.S.A. Tel: +13135778065, Fax: +13135772033, e-mail: dseparovic@wayne.edu

Key Words: Apoptosis, ceramide, ceramide synthase 1, dihydroceramide, PDT, sphingolipids, head and neck squamous carcinomas cells UM-SCC-22A.

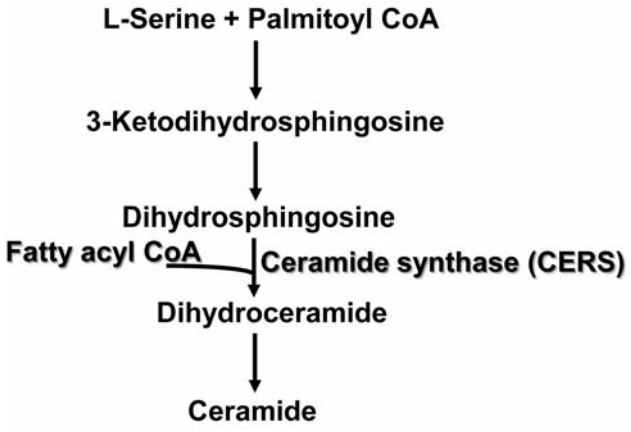

Figure 1. *The de novo sphingolipid biosynthesis pathway.*

PDT-induced apoptosis is unclear. In the current study, we explored the effects of *CERS1* knockdown on apoptosis and the sphingolipid profile post-Pc 4-PDT in UM-SCC-22A, a human head and neck squamous carcinoma cell line.

Materials and Methods

Materials. Pc 4, $HOSiPcOSi(CH_3)_2(CH_2)_3N(CH_3)_2$, was kindly supplied by Dr. Malcolm E. Kenney (Case Western Reserve University, Cleveland, OH, USA). Dulbecco's modified Eagle's medium (DMEM) and serum were from Invitrogen Life Sciences (Grand Island, NY, USA) and Hyclone (Logan, UT, USA), respectively. UM-SCC-22A, a human head and neck squamous carcinoma cell line from the hypopharynx (21, 22), was kindly supplied by Dr. Thomas Carey (University of Michigan, Ann Arbor, MI, USA).

Cell culture. UM-SCC-22A cells were grown in DMEM medium containing 10% fetal bovine serum, 1% non-essential amino acids, 100 units/ml penicillin, and 100 μg/ml streptomycin. Cells were maintained at 37˚C in an incubator with 5% CO_2 atmosphere, and were treated in the growth medium.

siRNA transfection and PDT treatment. The siRNA targeting the sequence AAG GTC CTG TAT GCC ACC AGT of human CERS1 was from Qiagen (Valencia, CA, USA) (12, 23). For control siRNA, AllStars Negative Control siRNA from Qiagen was used. UM-SCC-22A cells were transfected with double-strand siRNAs using Oligofectamine from Invitrogen Life Sciences, according to the manufacturer's instructions. To optimize the concentration of siCERS1, preliminary dose-response experiments (10-40 nM siCERS1) were carried out. As described previously (20), cells (1×10^6-2.5×10^6) were transfected with 25 nM of each siRNA. Twenty-four hours after transfection, cells were collected and seeded in fresh growth medium. Following overnight exposure to Pc 4 (250 and 500 nM), cells were irradiated with red light (2 mW/cm^2; λ_{max} ~670 nm) using a light-emitting diode array (EFOS; Mississauga, ON, Canada) at a fluence of 200 mJ/cm^2 at room temperature. Following PDT, cells were incubated at 37˚C for 2 or 24 h, were collected on ice and were processed for various analyses. For mass spectrometric analysis, cells were washed twice with cold phosphate-buffered saline, resuspended in a mixture of ethyl acetate/methanol (1:1, v/v), dried under nitrogen, and shipped overnight on dry ice to the Lipidomics Shared Resource (Medical University of South Carolina, Charleston, SC, USA) for further processing.

Sphingolipid analysis by quantitative high-performance liquid chromatography (HPLC)/mass spectrometry (MS). Following extraction, sphingolipids were separated by HPLC, introduced to an electrospray ionization source and were then analyzed by double MS using TSQ 7000 triple quadrupole mass spectrometer from Thermo-Fisher Scientific (Waltham, MA, USA), as described previously (24).

Immunoblotting. Following PDT, cells were collected, lysed in reducing Laemmli buffer, boiled and then subjected to sodium dodecyl sulfate polyacrylamide gel electrophoresis (SDS-PAGE) and western immunoblotting, as reported previously (16, 25). Equal protein loading was confirmed using anti-pan-actin and anti-HSP90. The following antibodies were obtained from Novus Biologicals (Littleton, CO, USA): anti-CERS1 and anti-CERS6 (mouse polyclonal each); anti-CERS2 (mouse monoclonal); anti-CERS5 (rabbit polyclonal). These antibodies were originally made by Abnova (Taipei City, Taiwan, ROC). Mouse monoclonal anti-HSP90 was from BD Biosciences (San Diego, CA, USA). Mouse monoclonal anti-pan-actin was from Neo Markers (Kalamazoo, MI, USA). Following visualization of blots using ECL Plus chemifluorescence kit and a STORM 860 imaging system (GE Healthcare, Piscataway, NJ, USA), they were quantified by ImageQuant 5.2 (GE Healthcare).

Caspase-3-like (DEVDase) activity assay. As described previously (20), following PDT, cell harvesting and cell lysis, DEVDase activity, was measured using a fluorogenic derivative of the tetrapeptide substrate *acetyl-Asp-Glu-Val-Asp-7-amino-4-methylcoumarin* (*Ac-DEVD-AMC*) from Enzo Life Sciences (Farmingdale, NY, USA) and an F-2500 spectrofluorometer (Hitachi; Dallas, TX, USA) (380 nm excitation, 460 nm emission).

Mitochondrial membrane depolarization measurement. The lipophilic cationic dye JC-1 (5,5',6,6'-tetrachloro-1,1'3,3'-tetraethylbenzimidazolylcarbocyanine iodide) was used to determine mitochondrial membrane potential by flow cytometry, as we described previously (17, 20, 26). Following PDT, cells were harvested and processed for flow cytometry according to the manufacturer's instructions (BD Biosciences, San Diego, CA, USA). ABD LSR II flow cytometer was used for analysis (BD Biosciences).

Apoptosis detection. As we showed previously (20, 26, 27), in order to detect apoptosis, the exposure of phosphatidylserine in the outer leaflet of the cell membrane and cell membrane integrity loss were measured using annexin V and DNA-binding propidium iodide (PI) fluorescent dyes, respectively. Early apoptotic (annexin V^+/PI^-) cells were distinguished from late apoptotic or necrotic cells (annexin V^+/PI^+). The kit was obtained from BD Biosciences and the flow cytometric protocol was followed, as described by the manufacturer.

Trypan blue dye exclusion assay. After PDT, cells were harvested, resuspended in cell growth medium, and diluted 1:1 with 0.4% trypan blue stain from Sigma-Aldrich (St. Louis, MO, USA). Stained and unstained cells were counted using a hemocytometer. Trypan blue-positive cells were designated as dead cells.

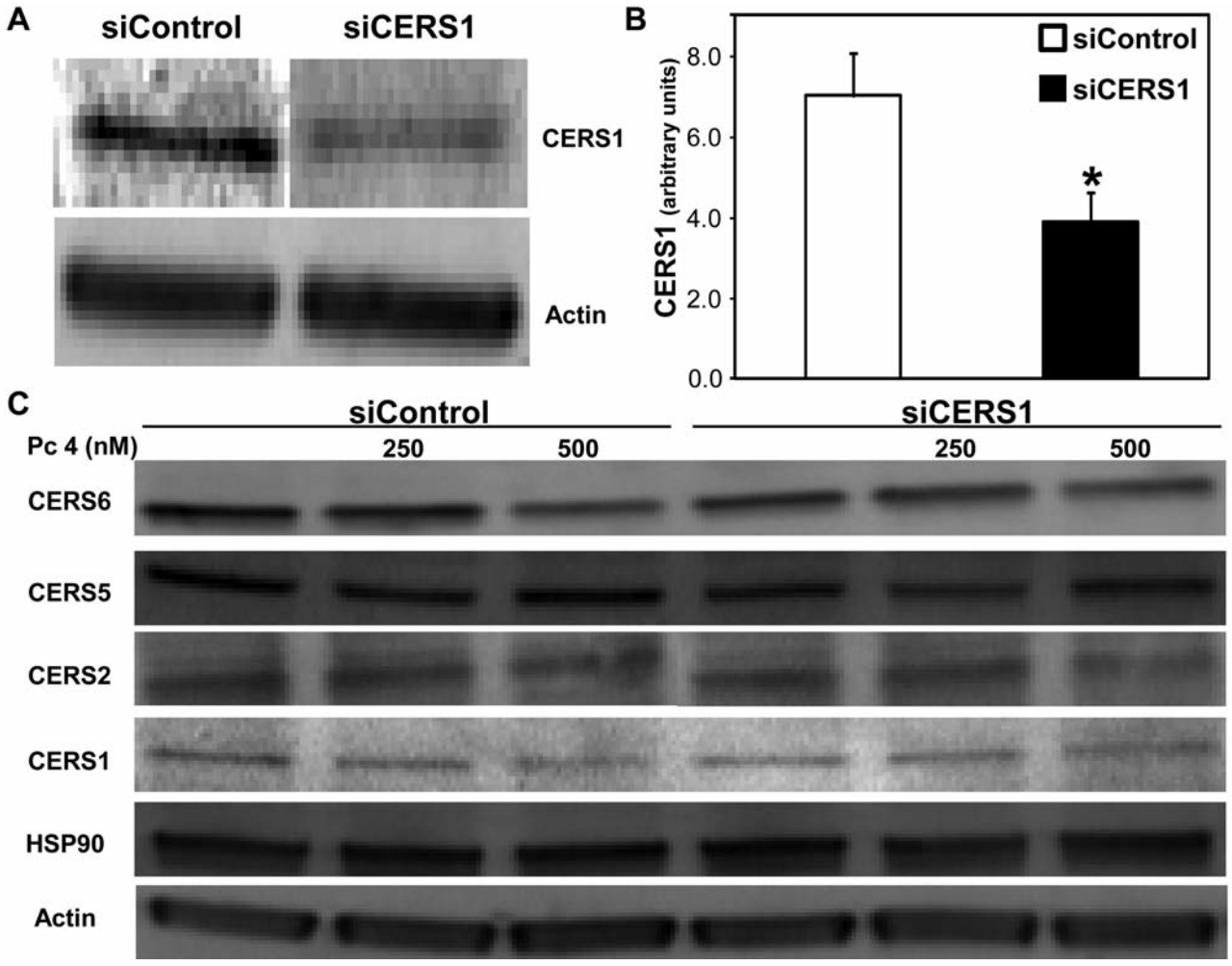

Figure 2. *Effect of ceramide synthase 1 (CERS1) knockdown and photodynamic therapy (PDT) on expression of ceramide synthases. UM-SCC-22A cells were transfected with siRNA targeted against non-targeted control (siControl; 25 nM) or CERS1 (siCERS6; 25 nM). Twenty-four hours after transfection, cells were collected and seeded in fresh growth medium. A and B: Cells were incubated at 37˚C for additional 24 hours prior to collection. C: After overnight exposure to the photosensitizer Pc 4 (250 and 500 nM), cells were irradiated with red light (2 mW/cm^2). Following PDT, cells were incubated at 37˚C for a further 2 h, collected on ice and processed for PAGE/Western immunoblotting. Equal protein loading was verified using anti-actin and anti-HSP90. A: Knockdown of CERS1 was confirmed in two independent experiments. B: CERS1 protein levels were quantified from the blots and expressed in arbitrary units. The data are shown as the mean±SEM, *p≤0.05, n=5-6. C: Western blots of CERS1, -2, -5 and -6 in siControl- and siCERS1-tranfected cells are shown. Representative blots from 2-5 independent determinations are shown.*

Statistical analysis. Following data collection, the mean value and the standard error of the untreated and each treated group were calculated for at least n=3. Data were analyzed for statistically significant differences ($p \leq 0.05$) between groups using the Student's *t*-test of unequal variance.

Results

Effect of CERS1 knockdown and PDT on ceramide synthase expression. To verify the down-regulation of CERS1 by RNA interference in UM-SCC-22A cells, protein expression levels were determined using immunoblotting. As shown in Figure 2A and B, CERS1 protein levels were reduced by 46% after *CERS1* knockdown. Following PDT (500 nM Pc 4 + 200 mJ/cm^2), the CERS1 protein was down-regulated in both siControl- and siCERS1-transfected cells.

To test for potential off-target effects, expression levels of CERS2, -5, and -6 were determined using immunoblotting. As shown in Figure 2C, expression of these CERSs was not affected by *CERS1* knockdown. The effect of PDT on the expression of other CERSs was similar in both siControl- and siCERS1-transfected cells.

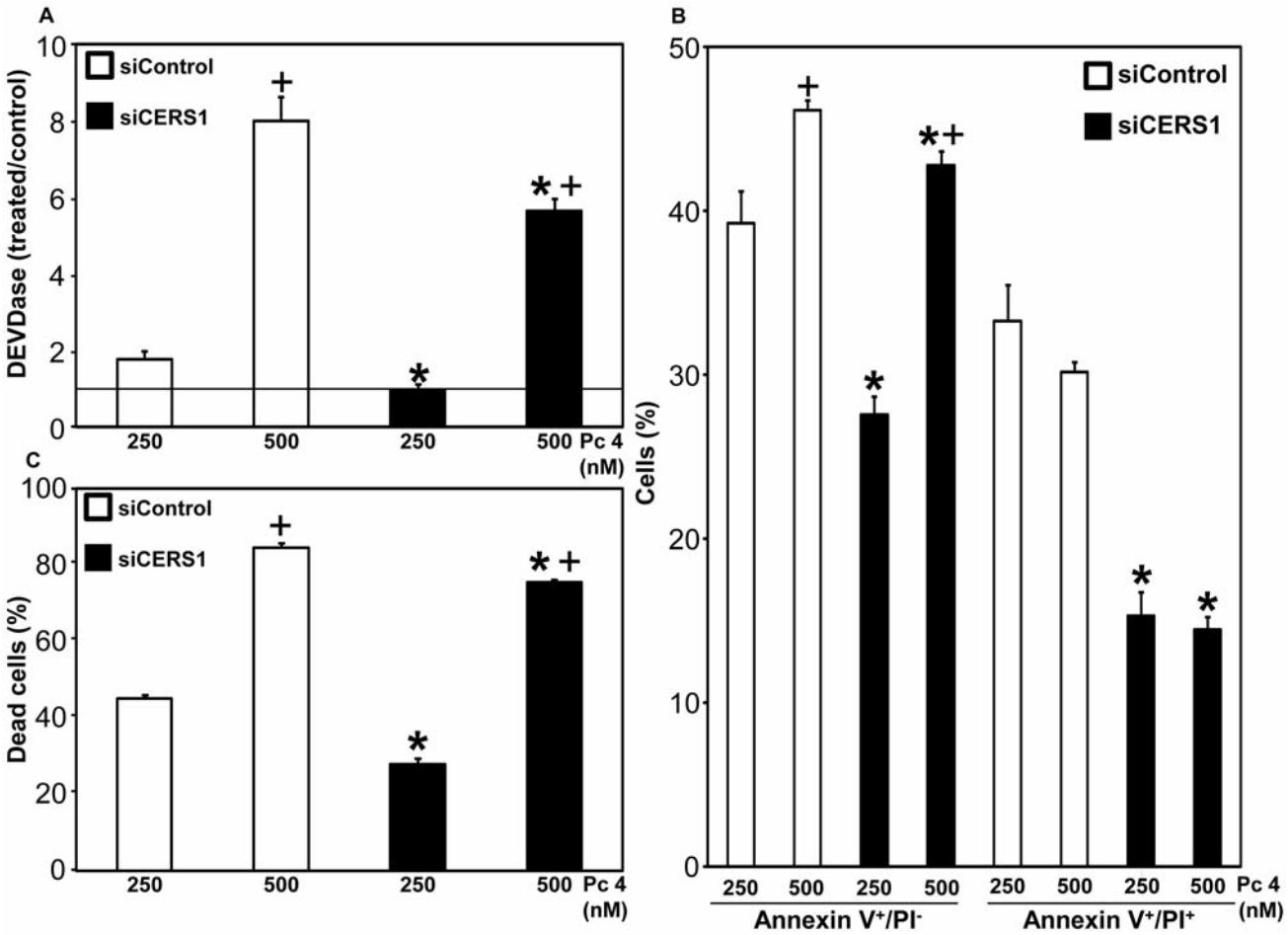

Figure 3. *Ceramide synthase 1 (CERS1) knockdown suppressed caspase-3-like (DEVDase) activation, apoptosis and cell death after photodynamic therapy (PDT). A: Following 2 h-incubation post-PDT, cells were collected, cell lysates were prepared and DEVDase activity was measured using acetyl-Asp-Glu-Val-Asp-7-amino-4-methylcoumarin (Ac-DEVD-AMC), as the fluorogenic substrate. B: Following 24 h-incubation post-PDT, cells were collected and processed for flow cytometry. Annexin V/propidium iodide (PI) staining was used to detect apoptosis. C: Following 24 h-incubation post-PDT, cells were collected, stained with trypan blue and counted. A: The data are expressed as ratios of PDT-treated versus untreated controls. In all panels, data are shown as the mean±SEM, n=3-11. The significance ($p \leq 0.05$) is indicated as follows: PDT-induced DEVDase activation, apoptosis and cell death were suppressed by CERS1 knockdown; +DEVDase activation, apoptosis and cell death was different at two PDT doses.*

CERS1 knockdown suppressed apoptosis and cell death without affecting the mitochondrial depolarization after PDT. The loss of mitochondrial membrane potential accompanies PDT-evoked apoptosis (17, 28). *CERS6* knockdown suppresses PDT-induced mitochondrial depolarization (20). We asked whether CERS1 affects apoptosis at the mitochondrial level after PDT. We found that PDT-induced mitochondrial depolarization was not modulated by *CERS1* knockdown (data not shown). The data suggest that CERS1 is not involved in mitochondrial apoptosis after PDT.

CERS6 knockdown inhibits PDT-induced apoptosis (20). The involvement of CERS1 in PDT-induced apoptosis is unknown. We first examined the effect of *CERS1* knockdown on DEVDase activity after PDT. We found that at 2 h after PDT, DEVDase activation was significantly inhibited by *CERS1* knockdown (Figure 3A). These findings support the involvement of CERS1 in the activation of DEVDase post-PDT.

We investigated the role of CERS1 in apoptosis after PDT using the apoptotic marker annexin V. Flow cytometric data revealed that *CERS1* knockdown led to significant reductions in the appearance of annexin V^+ and annexin V^+/PI^+ cells at 24 h after PDT (Figure 3B). These findings suggest that *CERS1* knockdown yields cells resistant to early and late apoptosis post-PDT.

To assess the effect of *CERS1* knockdown on short-term cell viability post-PDT, trypan blue dye exclusion assay was used. We found that following PDT, the appearance of trypan blue-positive cells was attenuated by *CERS1* knockdown at

24 h (Figure 3C). Thus, *CERS1* knockdown, similarly to *CERS6* knockdown (20), suppressed cytotoxicity after PDT.

Effect of CERS1 knockdown on the sphingolipid profile. *CERS6* knockdown is associated with changes in the sphingolipid profile both at rest and after PDT (20). To determine the effect of *CERS1* knockdown on the sphingolipid profile, resting levels of sphingolipids were measured by MS. *CERS1* knockdown significantly increased the levels of dihydrosphingosine, a CERS substrate. Out of all ceramides and dihydroceramides tested, the only significant change evoked by *CERS1* knockdown was an increase in the levels of C16-ceramide and C16-dihydroceramide (Table I).

We then explored the effect of PDT on the sphingolipid profile in cells transfected with siControl- or siCERS1. The data presented here were obtained at 2 h post-PDT. *CERS1* knockdown significantly suppressed global accumulation of ceramides and dihydroceramides after PDT (Figure 4A).

Among all ceramides and dihydroceramides tested, PDT induced the greatest increase in C18-dihydroceramide (Figure 4B). The 60-fold increase in C18-dihydroceramide after PDT was substantially reduced by *CERS1* knockdown. *CERS1* knockdown also significantly reduced the accumulation of the following dihydroceramides after PDT: C14-, C16-, C18:1-, C22-, C22:1-, C24-, and C26:1-dihydroceramide. Furthermore, *CERS1* knockdown significantly suppressed PDT-induced accumulation of the following ceramides: C18-, C18:1-, and C20-ceramide (Figure 4B). The effect of *CERS1* knockdown on accumulation of other ceramides and dihydroceramides did not correlate with reduced functional responses (not shown). Taken together, *CERS1* knockdown was associated with selective decreases in individual ceramides and dihydroceramides, as well as with global decreases in ceramides and dihydroceramides after PDT.

Table I. *Resting sphingolipid levels in UM-SCC-22A cells.*

Sphingolipid	pmol/mg±SEM	
	siControl	siCERS1
Dihydrosphingosine	5.9±0.5	9.3±0.8*
C14-DHCeramide	1.5±0.4	2.3±0.3
C16-DHCeramide	18.3±2.4	27.6±0.9*
C18-DHCeramide	2.2±0.4	2.7±0.3
C18:1-DHCeramide	0.5±0.2	0.8±0.2
C20-DHCeramide	11.2±1.4	8.8±0.8
C20:1-DHCeramide	1.7±0.2	1.4±0.2
C22-DHCeramide	2.3±0.3	3.2±0.4
C22:1-DHCeramide	0.9±0.1	0.8±0.1
C24-DHCeramide	7.0±1.0	10.1±1.2
C24:1-DHCeramide	4.9±0.9	5.2±0.3
C26-DHCeramide	1.3±0.2	1.3±0.2
C26:1-DHCeramide	0.6±0.0	0.9±0.1
C14-Ceramide	22.9±2.7	24.9±2.4
C16-Ceramide	200.6±16.2	252.2±13.3*
C18-Ceramide	17.7±2.0	17.3±1.3
C18:1-Ceramide	6.8±0.4	6.5±0.3
C20-Ceramide	14.9±1.9	14.0±1.2
C20:1-Ceramide	1.8±0.3	2.3±0.3
C22-Ceramide	38.8±4.8	36.9±2.9
C22:1-Ceramide	19.6±1.7	17.1±1.4
C24-Ceramide	151.5±19.8	149.1±14.2
C24:1-Ceramide	138.4±17.4	130.5±11.4
C26-Ceramide	31.9±4.9	28.3±2.8
C26:1-Ceramide	22.5±2.8	18.6±2.3

Resting levels of sphingolipids (pmol/mg) from untreated UM-SCC-22A cells are shown as the mean±SEM (n=3-5). *Denotes a value significantly different from that of the control.

Discussion

The key findings of our present study are that *CERS1* knockdown is associated with global and selective decreases in ceramides and dihydroceramides, in particular C18-, C18:1- and C20-ceramide, leading to suppression of apoptosis post-PDT. Our present data strongly support a role of CERS1 and sphingolipids in apoptotic resistance to PDT. Similarly, down-regulation of CERS1 inhibits imatinib-induced cell death (13) and renders head and neck squamous carcinoma cells resistant to anticancer agents (12). We have recently shown that *CERS6* knockdown supresses apoptosis after PDT (20). Compared to *CERS6* knockdown, *CERS1* knockdown was unable to modulate mitochondrial depolarization and to suppress apoptosis post-PDT to the same extent. Regardless, we have demonstrated that CERS1 knockdown, similar to CERS6 knockdown, leads to apoptotic resistance in UM-SCC-22A cells post-PDT.

Mammalian CERS1 has been shown to utilize C18-CoA preferentially (5, 10), and to a lesser extent, C18:1- and C20-CoA (5, 10, 12, 29). However, specificity of CERS1 for these substrates was not observed following CERS1 knockdown. In the absence of differences in expressions of other CERSs between cells transfected with control- or CERS1-siRNA, the observed lack of specificity for C18-ceramide by *CERS1* knockdown suggests relaxation of substrate specificity of the enzyme (9). Alternatively, low levels of CERS1 expression and C18-ceramide in head and neck squamous carcinoma cells (14) might counteract the ability of *CERS1* knockdown to lower C18-ceramide levels any further. Nevertheless, a significant increase in the levels of dihydrosphingosine, a CERS1 substrate, is consistent with the idea of CERS1 knockown.

The involvement of CERS1 in PDT-induced changes in the sphingolipid profile is supported by the following data: C18-, C18:1- and C20-ceramide were the only ceramides that were significantly reduced by the CERS1 knockdown; the levels of C18- and C18:1-dihydroceramide were also substantially suppressed. However, specificity of CERS1 for PDT-induced changes in the sphingolipid profile was only partial, since

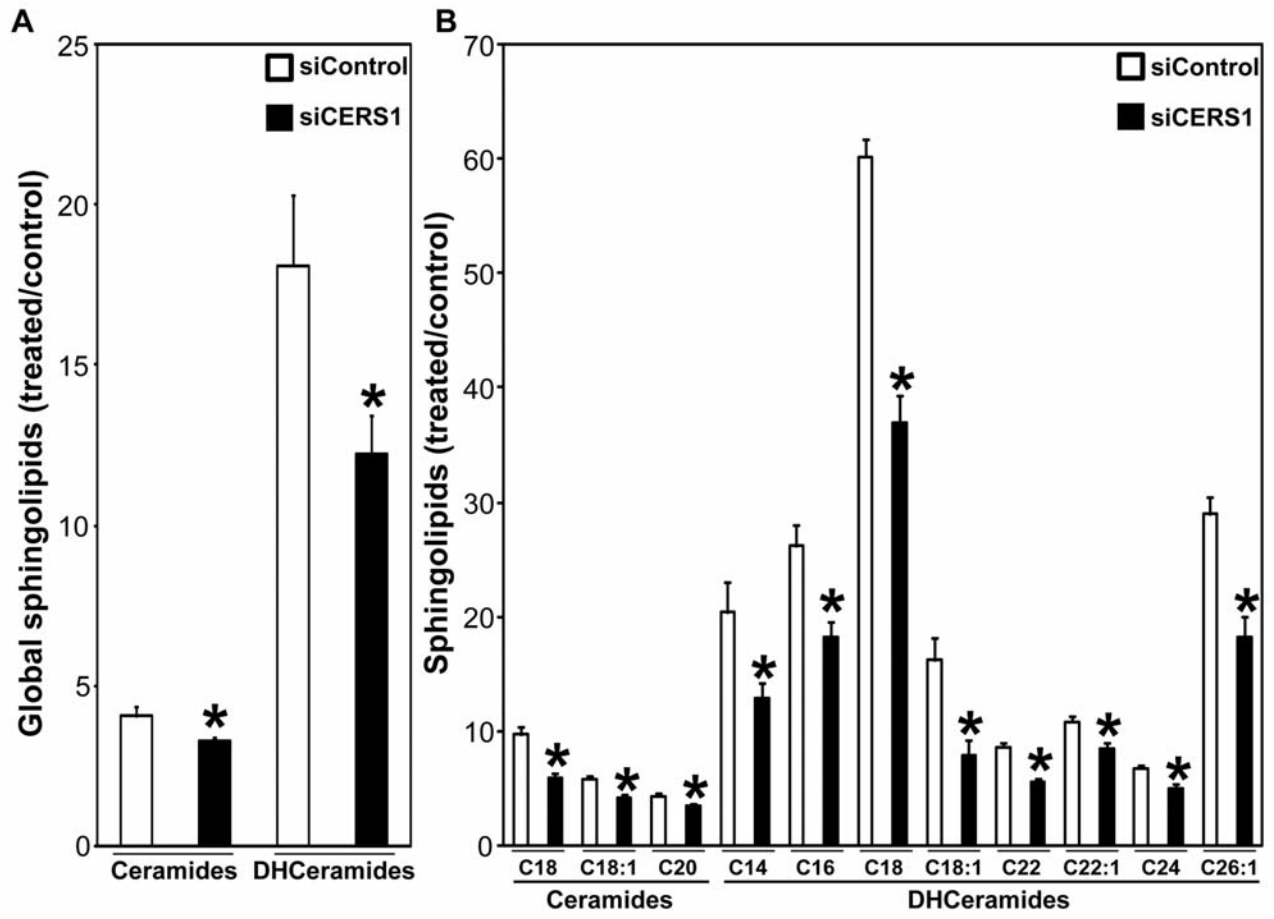

Figure 4. *Effect of ceramide synthase 1 (CERS1) knockdown on photodynamic therapy (PDT)-induced accumulation of global (A) or individual (B) ceramides and dihydroceramides (DHceramides). Following 2 h-incubation post-PDT (500 nM Pc 4 + 200 mJ/cm^2), cells were collected and processed for mass spectrometry. The data are expressed as ratios of PDT-treated versus untreated controls. In both panels, the data are shown as the mean±SEM, n=3-5. *Indicates that CERS1 knockdown suppressed PDT-induced accumulation of corresponding ceramides or dihydroceramides at p≤0.05.*

CERS1 knockdown evoked significant decreases in global ceramides and dihydroceramides. Moreover, the levels of C14-, C16-, C22-, C22:1, C24- and C26:1-dihydroceramide were also reduced by CERS1 knockdown post-PDT. In the absence of differences in expressions of other CERSs between cells transfected with control- or CERS1-siRNA, post-PDT observed changes in global ceramides, global and individual dihydroceramides by CERS1 knockdown suggest partial substrate specificity of the enzyme after PDT (9).

In summary, our present study indicates that CERS1 controls apoptotic susceptibility to PDT in part *via* the *de novo* production of C18- and C20-ceramide. These novel findings support the idea that alterations in CERS1 expression might be utilized therapeutically to control resistance to PDT.

Acknowledgements

This work was supported by U.S. Public Health Service Grant R01 CA77475 from the National Cancer Institute, National Institutes of Health (DS) and the Veterans Administration Merit Awards from RR&D and BLRD programs (TIG). The MS-related work was performed by the Lipidomics Shared Resource (Medical University of South Carolina), supported by NCI grants: IPO1CA097132 and P30 CA 138313 and NIH/NCRR SC COBRE Grant P20 RR017677. Laboratory space for the Lipidomics Shared Resource was supported by the NIH, grant C06 RR018823 from the Extramural Research Facilities Program of the National Center for Research Resources. We thank Drs. Besim Ogretmen and Can Emre Senkal for helpful discussions over the manuscript.

References

1 Levy M and Futerman AH: Mammalian ceramide synthases. IUBMB Life *62*: 347-356, 2010.

2 Henry B, Moller C, Dimanche-Boitrel MT, Gulbins E and Becker KA: Targeting the ceramide system in cancer. Cancer Lett 2011, doi: 10.1016/j.canlet.2011.07.010.

3 Mullen TD, Hannun YA and Obeid LM: Ceramide synthases at the centre of sphingolipid metabolism and biology. Biochem J *441*: 789-802, 2012.

4 Riebeling C, Allegood JC, Wang E, Merrill AH Jr. and Futerman AH: Two mammalian longevity assurance gene (LAG1) family members, TRH1 and TRH4, regulate dihydroceramide synthesis using different fatty acyl-CoA donors. J Biol Chem *278*: 43452-43459, 2003.
5 Mizutani Y, Kihara A and Igarashi Y: Mammalian Lass6 and its related family members regulate synthesis of specific ceramides. Biochem J *390*: 263-271, 2005.
6 Mizutani Y, Kihara A, Chiba H, Tojo H and Igarashi Y: 2-Hydroxy-ceramide synthesis by ceramide synthase family: enzymatic basis for the preference of FA chain length. J Lipid Res *49*: 2356-2364, 2008.
7 Laviad EL, Albee L, Pankova-Kholmyansky I, Epstein S, Park H, Merrill AH Jr. and Futerman AH: Characterization of ceramide synthase 2: Tissue distrubution, substrate specificity, and inhibition by sphingosine 1-phosphate. J Biol Chem *283*: 5677-5684, 2008.
8 Tidhar R, Ben-Dor S, Wang E, Kelly S, Merrill AH Jr. and Futerman AH: The acyl chain specificity of ceramide synthases is determined within a region of 150 residues in the Tram-Lag-CLN8 (TLC) domain. J Biol Chem *287*: 3197-3206, 2012.
9 Hannun YA and Obeid LM: Many ceramides. J Biol Chem *286*: 27855-27862, 2011.
10 Venkataraman K, Riebeling C, Bodennec J, Riezman H, Allegood JC, Sullards MC, Merrill AH Jr. and Futerman AH: Upstream of growth and differentiation factor 1 (Uog1), a mammalian homolog of the yeast longevity assurance gene 1 (lag1), regulates N-stearoyl-sphinganine (C18-(dihydro)ceramide) synthesis in a fumonisin B1-independent manner in mammalian cells. J Biol Chem *277*: 35642-35649, 2002.
11 Min J, Mesika A, Sivaguru M, Van Veldhoven PP, Alexander H, Futerman AH and Alexander S: (Dihydro)ceramide synthase 1 regulated sensitivity to cisplatin is associated with the activation of p38 mitogen-activated protein kinase and is abrogated by sphingosine kinase 1. Mol Cancer Res *5*: 801-812, 2007.
12 Senkal CE, Ponnusamy S, Rossi MJ, Bialewski J, Sinha D, Jiang JC, Jazwinski SM, Hannun YA and Ogretmen B: Role of human longevity assurance gene 1 and C18-ceramide in chemotherapy-induced cell death in human head and neck squamous cell carcinomas. Mol Cancer Ther *6*: 712-722, 2007.
13 Baran Y, Salas A, Senkal CE, Gunduz U, Bielawski J, Obeid LM and Ogretmen B: Alterations of ceramide/sphingosine 1-phosphate rheostat involved in the regulation of resistance to imatinib-induced apoptosis in K562 human chronic myeloid leukemia cells. J Biol Chem *282*: 10922-10934, 2007.
14 Koybasi S, Senkal CE, Sundararaj K, Spassieva S, Bielawski J, Osta W, Day TA, Jiang JC, Jazwinski SM, Hannun YA, Obeid LM and Ogretmen B: Defects in cell growth regulation by C18:0-ceramide and longevity assurance gene 1 in human head and neck squamous cell carcinomas. J Biol Chem *279*: 44311-44319, 2004.
15 Wispriyono B, Schmelz E, Pelayo H, Hanada K and Separovic D: A role for the *de novo* sphingolipids in apoptosis of photosensitized cells. Exp Cell Res *279*: 153-165, 2002.
16 Dolgachev V, Farooqui MS, Kulaeva OI, Tainsky MA, Nagy B, Hanada K and Separovic D: *De novo* ceramide accumulation due to inhibition of its conversion to complex sphingolipids in apoptotic photosensitized cells. J Biol Chem *279*: 23238-23249, 2004.
17 Dolgachev V, Nagy B, Taffe B, Hanada K and Separovic D: Reactive oxygen species generation is independent of *de novo* sphingolipids in apoptotic photosensitized cells. Exp Cell Res *288*: 425-436, 2003.
18 Agostinis P, Berg K, Cengel KA, Foster TH, Girotti AW, Gollnick SO, Hahn SM, Hamblin MR, Juzeniene A, Kessel D, Korbelik M, Moan J, Mroz P, Nowis D, Piette J, Wilson BC and Golab J: Photodynamic therapy of cancer: an update. CA Cancer J Clin *61*: 250-281, 2011.
19 Henderson BW, Gollnick SO, Snyder JW, Busch TM, Kousis PC, Cheney RT and Morgan J: Choice of oxygen-conserving treatment regimen determines the inflammatory response and outcome of photodynamic therapy of tumors. Cancer Res *64*: 2120-2126, 2004.
20 Separovic D, Breen P, Joseph N, Bielawski J, Pierce JS, Van B E and Gudz TI: Ceramide synthase 6 knockdown suppresses apoptosis after photodynamic therapy in human head and neck squamous carcinoma cells. Anticancer Res *32*: 753-760, 2012.
21 Brenner JC, Graham MP, Kumar B, Saunders LM, Kupfer R, Lyons RH, Bradford CR and Carey TE: Genotyping of 73 UM-SCC head and neck squamous cell carcinoma cell lines. Head Neck *32*: 417-426, 2010.
22 Zhu Z, Xu X, Yu Y, Graham M, Prince ME, Carey TE and Sun D: Silencing heat shock protein 27 decreases metastatic behavior of human head and neck squamous cell cancer cells in vitro. Mol Pharm *7*: 1283-1290, 2010.
23 Senkal CE, Ponnusamy S, Bielawski J, Hannun YA and Ogretmen B: Antiapoptotic roles of ceramide-synthase-6-generated C16-ceramide *via* selective regulation of the ATF6/CHOP arm of ER-stress-response pathways. FASEB J *24*: 296-308, 2010.
24 Separovic D, Semaan L, Tarca AL, Awad Maitah MY, Hanada K, Bielawski J, Villani M and Luberto C: Suppression of sphingomyelin synthase 1 by small interference RNA is associated with enhanced ceramide production and apoptosis after photodamage. Exp Cell Res *314*: 1860-1868, 2008.
25 Separovic D, Kelekar A, Nayak AK, Tarca AL, Hanada K, Pierce JS and Bielawski J: Increased ceramide accumulation correlates with down-regulation of the autophagy protein ATG-7 in MCF-7 cells sensitized to photodamage. Arch Biochem Biophys *494*: 101-105, 2010.
26 Separovic D, Saad ZH, Edwin EA, Bielawski J, Pierce JS, Van Buren E and Bielawska A: C16-ceramide analog combined with Pc 4 photodynamic therapy evokes enhanced total ceramide accumulation, promotion of DEVDase activation in the absence of apoptosis, and augmented overall cell killing. J Lipids *2011*: 1-9, 2011.
27 Separovic D, Mann KJ and Oleinick NL: Association of ceramide accumulation with photodynamic treatment-induced cell death. Photochem Photobiol *68*: 101-109, 1998.
28 Lam M, Oleinick NL and Nieminen AL: Photodynamic therapy-induced apoptosis in epidermoid carcinoma cells. Reactive oxygen species and mitochondrial inner membrane permeabilization. J Biol Chem *276*: 47379-47386, 2001.
29 Spassieva S, Seo JG, Jiang JC, Bielawski J, Alvarez-Vasquez F, Jazwinski SM, Hannun YA and Obeid LM: Necessary role for the Lag1p motif in (dihydro)ceramide synthase activity. J Biol Chem *281*: 33931-33938, 2006.

Received May 2, 2012
Revised May 28, 2012
Accepted May 29, 2012